

**N86-19734****THERMAL-CAPILLARY MODEL FOR CZOCHRALSKI  
GROWTH OF SEMICONDUCTOR MATERIALS**

J.J. Derby and R.A. Brown

Department of Chemical Engineering  
Massachusetts Institute of Technology  
Cambridge, Massachusetts 02139**Introduction and Methodology**

Over 80 per cent of the silicon used by the electronics industry is grown from the melt by the Czochralski (CZ) crystal growth process, which is depicted schematically in Fig. 1. A single crystal boule is slowly pulled from a pool of melt maintained by heating the outside of the crucible. Surface tension acts against the force of gravity to form a meniscus connecting the the growing crystal to the surface of the melt pool. The precise temperature gradient needed to sustain the solidification of nearly perfect crystalline solid is maintained by a cooler ambient above the crucible. The crystal and crucible are rotated to minimize thermal asymmetry in the system. In addition, as the melt level drops during growth, the crucible is raised by movement of the pedestal so that the solidification front remains in a specified region of the heater.

Capillarity and heat transfer determine the shape and stability of crystals grown by the Czochralski method. We describe the solution of the first quasi-steady, thermal-capillary model of the CZ growth process which directly predicts the dependence of the crystal radius, melt-solid interface, and melt/gas meniscus on growth parameters and thermal boundary conditions in the furnace. The equations governing heat transfer are presented in Fig. 2., and the expressions for determining the radius and interface location are shown in Fig. 3. We model heat transfer in the system as conduction-dominated and include latent heat generation at the solidification interface. Radiation and convection accounts for heat exchange between the melt and crystal and the thermal surroundings. The thermal boundary conditions used in the calculations presented here represent an idealized, but qualitatively realistic thermal environment for CZ crystal growth. The heating of the melt through the crucible is modeled by specifying the temperature of the melt adjacent to the crucible wall as a constant without coupling this value to the actual power input to the crucible from the surrounding heater. Heat flows out of the melt through the bottom of the crucible, according to a specified heat transfer coefficient set to model energy loss to the pedestal and the surroundings. By itself, this heat transfer system represents a slightly nonlinear conduction-radiation problem and its solution would be straightforward except that the shape of the melt and crystal are unknown and are a part of the solution.

The locations of the interfaces are coupled to the heat transfer in the system by setting the shapes of the regions for conduction and by determining the surface areas for radiative and convective exchange with the ambient.

The melt/solid interface is determined by the location of the melting point isotherm. The shape of the melt meniscus is found from the Young-Laplace equation of capillary statics, the condition for three-phase contact at the melt/solid/gas tri-junction, the wetting condition at the crucible wall, and by the specification of the instantaneous volume of the melt. The radius of the crystal is determined so that the three-phase (melt/crystal/gas) equilibrium contact angle for growth is satisfied (Surek and Chalmers 1975).

These relations form a complete set of coupled partial differential equations for this complex nonlinear free-boundary problem. Only Ettouney et al. (1983) have solved a thermal-capillary model with a similar degree of complexity. As detailed in Fig. 4., We solve the field and boundary equations simultaneously by a finite-element/Newton scheme for the temperature field in melt and crystal, the shapes of the meniscus and melt-solid interface, and the radius of the crystal. Besides giving quadratic convergence in each of these unknowns, the Newton method is the basis for computer-implemented analyses of parametric sensitivity and stability (Yamaguchi et al. 1984). The details of the finite element algorithm are presented in a recent manuscript (Derby et al. 1985) for the modeling of liquid encapsulated Czochralski growth of gallium arsenide.

## Results

Results for the thermophysical properties characteristic of CZ Silicon growth in a small-scale system are shown in Fig. 5. along with a specified ambient temperature distribution. On the left representative isotherms are shown for the melt and crystal. Note that heat flows into the melt from the crucible wall and exits the melt both upward through the surface of the melt and through the crystal and downward out of the bottom of the crucible. The shape of the meniscus is shown along with the melt/solid interface which is concave into the crystal. For this set of parameters, the resultant crystal radius was 3.8 cm. On the right, the ambient temperature distribution for this case is shown. The almost step decrease in the surrounding temperature field that occurs above the top of the hot crucible was modeled by the ambient temperature profile shown in Fig. 5. The hot crucible has an increasingly important effect on the crystal size as the melt level drops and the outer crystal surface directly views this distribution. Similar ambient temperature distributions were used for the decreasing melt volume calculations of Figs. 10., 11., and 12.

The response of the system to changes in the steady-state growth rate is detailed in Fig. 6. as the pull rate, represented by the dimensionless Peclet number, is varied from 0-20 cm/hr ( $0 \leq Pe \leq 0.4$ ). All other parameters were held constant and the ambient distribution was taken to be uniform at 1262K. The crystal radius decreased with increasing pull rate because of the increased latent heat release at the interface. This effect has been observed experimentally. The release of latent heat also was responsible for the increasing curvature of the solidification interface. At higher growth rates the interface became increasingly concave into the crystal.

Some computational aspects of these calculations are presented in Figs. 7 and 8. The converged finite-element meshes for each of the calculations

are shown in Fig. 8. Meshes with 76 element were used in all calculations presented in this report. The mesh follows the shape and position of the changing interfaces for each case. Since the mesh was based on the location of the free-boundaries, it converged as part of the entire solution with every iteration. The iteration histories for these runs is detailed in Fig. 8. The convergence was quadratic, as expected for full Newton's method; see Ettouney and Brown (1983).

Calculations are presented in Fig 9. for different equilibrium growth angles for the wetting of the crystal by the melt. The angle is varied from the reported 11 degree value for silicon to 45 and 90 degrees. There were two major effects: the crystal radius decreased with increasing angle, and the shape of the melt-solid interface changed from concave into the crystal to convex into the melt as the angle increased from 11 to 90 degrees. The last case for an equilibrium angle of 90 degrees corresponded to the assumption used by most previous investigators of a flat melt surface joining the crystal at right angles. This simplification obviously lead to erroneous results. Accurate modeling of heat flow in this region necessitates inclusion of the melt meniscus and the proper equilibrium angle.

The next series of figures represents the interaction of the temperature field and interfaces with the melt volume. Several effects are present as the melt level drops. The amount of heat entering the melt from the crucible sides decreased because the surface area in contact with the wall decreased. Also, the heat loss out of the bottom of the crucible was increasingly important in the shallower melt, and the hot crucible wall was exposed. The exposed wall allowed for radiative heat transfer from the hot crucible wall directly into the growing crystal. First, we examine only the effect of the dropping melt level without the complicating effects of radiative heat transfer. The case of decreasing melt volume with an axially uniform ambient temperature of 1262 K is shown in Fig. 10. Since the amount of heat entering the melt decreased as the melt level drops, the radius of the crystal increased. The effect of the heat loss through the bottom of the crucible was manifested in a change of the interface shape from concave to sigmoidal. This transition is known as interface flipping and commonly has been attributed to transitions in the natural convection within the melt. Since our calculations are for a conduction-dominated system, interface flipping was caused solely by conductive heat losses through the melt and the changing shape of the melt pool. Another related effect of the crucible heat loss was the formation of a section of undercooled melt at the bottom of the crucible for the shallow melt depth ( $V_m=0.5\pi$ ). In practice, this region would be a small cap of solid silicon at the bottom of the crucible which can grow large enough with decreasing melt depth to touch the upper melt/solid interface. This is occasionally observed in practice, and is known as "crystal bumping".

When we add radiation from the exposed wall in the form of the specified axial temperature distribution discussed previously, we get the situations depicted in Figs. 11. and 12. Even though the heat flow into the melt decreased with the dropping melt, the radiative transfer of heat from the exposed wall into the crystal can prevent the growth in the radius of the crystal as the melt level dropped. This effect is seen for the case with melt volume  $V_m=0.5\pi$  for the shallow crucible in Fig. 11. and for both cases

for the deep crucible in Fig. 12. Radiation from the crucible wall to the crystal is so overpowering for the deeper crucible case of Fig. 12 that a non-zero crystal radius did not exist for the  $V_m=0.5\pi$  case. Radiative interchange between wall and crystal also magnified the interface flipping effect. With heat entering the side of the crystal, the melt/solid interface was pushed even further into the melt. The solid cap at the bottom of the crucible was present for the melt volume  $V_m=0.5\pi$  shown in Fig. 11.

The changes in radius for decreasing melt volume are shown together in Fig. 13. For the uniform ambient, the crystal radius increased steadily with decreasing melt volume. When an ambient temperature distribution was introduced to include the crucible wall the increasing effect of radiation from the exposed wall the radius show either a maximum with decreasing volume or decreased monotonically, depending on the depth of the crucible. For the shallow crucible, the crystal radius initially increased as the melt dropped, but decreased as more of the crucible wall was exposed to the view of the crystal. This effect is even more dramatic for the deep crucible: the radius decreased from the start and rapidly melted away so that no steady-state growth was possible after some minimum volume was reached. This last effect is often seen in practice where the crystal becomes very difficult to grow as the melt level drops below some critical value.

### Summary

We have demonstrated the success of efficiently calculating the temperature field, crystal radius, melt meniscus, and melt/solid interface in the Czochralski crystal growth system by full finite-element solution of the governing thermal-capillary model. The model predicts realistic response to changes in pull rate, melt volume, and the thermal field. The experimentally observed phenomena of interface flipping, bumping, and the difficulty maintaining steady-state growth as the melt depth decreases are explained by model results. These calculations will form the basis for the first quantitative picture of CZ crystal growth. The accurate depiction of the melt meniscus is important in calculating the crystal radius and solidification interface. The sensitivity of our results to the equilibrium growth angle place doubt on less sophisticated attempts to model the process without inclusion of a the meniscus.

Quantitative comparison with experiments should be possible once more representation of the radiation and view factors in the thermal system and the crucible are included. Extensions of our model in these directions are underway.

## References

Derby, J.J., Brown, R.A., Geyling, F.T., Jordan, A.S., and Nikolakopoulou, G.A., *J. Electrochem. Soc.* to appear, Feb. (1985).

Ettouney, H.M. and Brown, R.A., *J. Computat. Phys.* **49**, 118 (1983).

Ettouney, H.M., Brown, R.A., and Kalejs, J.P., *J. Crystal Growth* **62**, 230 (1983).

Surek, T. and Chalmers, B., *J. Crystal Growth* **29** 1 (1975).

Yamaguchi, Y., Chang, C.J., and Brown, R.A., *Philos. Trans. R. Soc. Lond.* **312** 520 (1984).

## Nomenclature

- $Bi_j$ , Biot number =  $\hat{h}_j R_C / k_S$  for surface  $j$ ;
- $Bo$ , Bond number =  $g R_C^2 \rho / \sigma$ ;
- $C_p$ , heat capacity [J/kgK];
- $\underline{e}_z$ , unit axial vector;
- $g$ , gravitational constant [m/s<sup>2</sup>];
- $\hat{h}_j$ , heat transfer coefficient for surface  $j$  [W/m<sup>2</sup>K];
- $\bar{H}_i$ , height of interface  $i$  from bottom of crucible [m];
- $h_i$ , dimensionless interface heights =  $\bar{h}_i / R_C$ ;
- $k$ , thermal conductivity [W/mK];
- $K_i$ , temperature-dependent thermal conductivity ratio =  $k_i / k_S$  for region  $i$ ;
- $\underline{n}_i$ , normal vector to surface  $i$ ;
- $Pe$ , Peclet number =  $V_p R_C \rho_S C_{pS} / k_S$ ;
- $\bar{r}$ , radial coordinate measured from center of crucible [m];
- $r$ , dimensionless radial coordinate =  $\bar{r} / R_C$ ;
- $\bar{R}$ , crystal radius [m];
- $R$ , dimensionless crystal radius =  $\bar{R} / R_C$ ;
- $R_C$ , crucible radius [m];
- $Ra_i$ , Radiation number =  $\sigma^* i R_C T_f^3 / k_S$  for surface  $i$ ;
- $S$ , Stefan number =  $H_f / C_{pS} T_f$ ;
- $T$ , temperature [K];
- $T_f$ , solidification temperature [K];
- $\bar{V}_m$ , volume of melt [m<sup>3</sup>];
- $V_m$ , dimensionless volume of melt =  $\bar{V}_m / R_C^3$ ;
- $V_p$ , steady-state crystal pull rate [m/s];
- $\bar{z}$ , axial coordinate measured from bottom of crucible [m];
- $z$ , dimensionless axial coordinate =  $\bar{z} / R_C$ ;

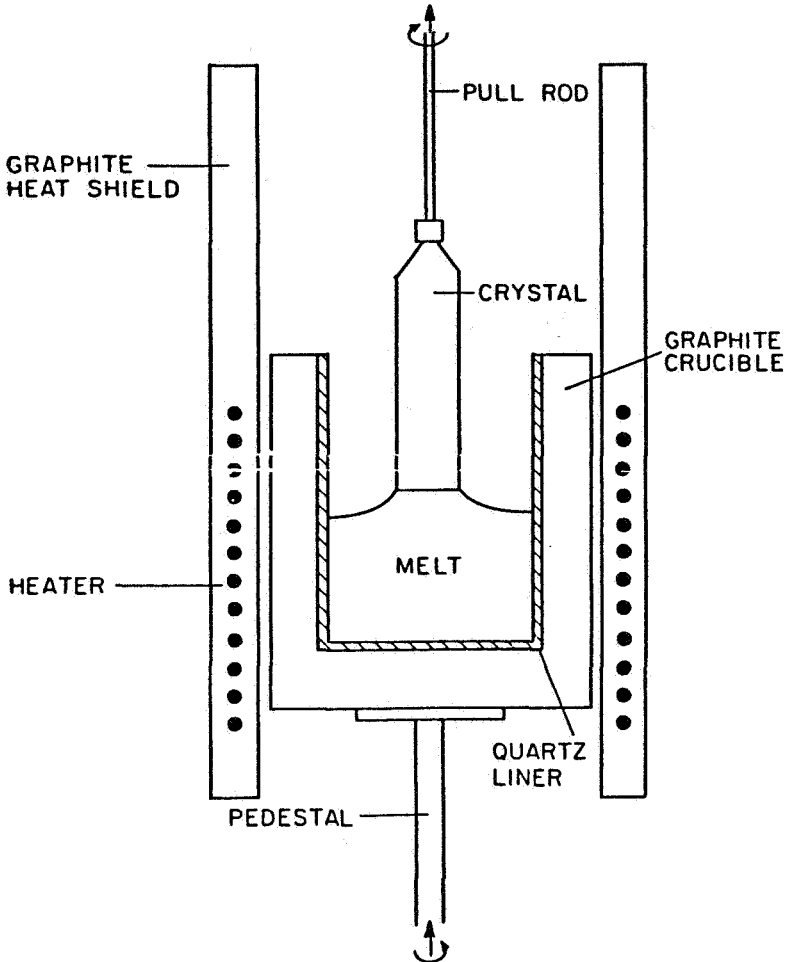
### Greek symbols

- $H_f$ , heat of fusion [J/kg-mole];
- $\rho$ , density difference across melt meniscus;
- $\epsilon_j$ , emissivity of surface  $j$ ;
- $\lambda_i$ , dimensionless reference pressure =  $P_{i,datum} / \rho_i g R_c$ ;
- $\phi$ , equilibrium wetting angle;
- $\rho$ , density [kg/m<sup>3</sup>];
- $\sigma$ , surface tension [J/m];
- $\sigma^*$ , Stefan-Boltzmann constant [W/m<sup>2</sup>K<sup>4</sup>];
- $\theta$ , dimensionless temperature =  $T/T_f$ ;

### Subscripts

- a, ambient;
- c, crucible;
- i,j, numerical indices denoting surface, domain, or equation;
- m, melt;
- s, solid.

# Czochralski Crystal Growth





# Steady-State Thermal-Capillary Model

## AXISYMMETRIC CONDUCTION-DOMINATED HEAT TRANSFER

$$\nabla \cdot K_m(\theta) \nabla \theta = 0 \quad (\text{Melt})$$

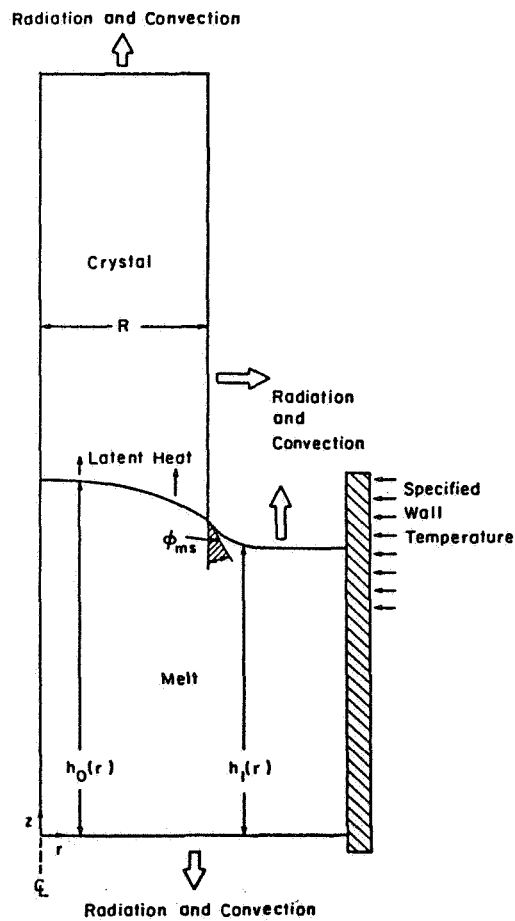
$$\nabla \cdot K_s(\theta) \nabla \theta - \rho_s (\mathbf{g} \cdot \nabla \theta) = 0 \quad (\text{Crystal})$$

## THERMAL BOUNDARY CONDITIONS

at melt-solid interface  $\theta_s = \theta_m = 1$   
 $K_m (\mathbf{n} \cdot \nabla \theta_m) - K_s (\mathbf{n} \cdot \nabla \theta_s) = \rho_s S (\mathbf{n} \cdot \mathbf{g}_z)$

at external surfaces  $-K (\mathbf{n} \cdot \nabla \theta) = Bi(\theta - \theta_a) + Ra(\theta^4 - \theta_a^4)$

at crucible inner wall  $\theta(r, z) = \theta_c(r, z)$



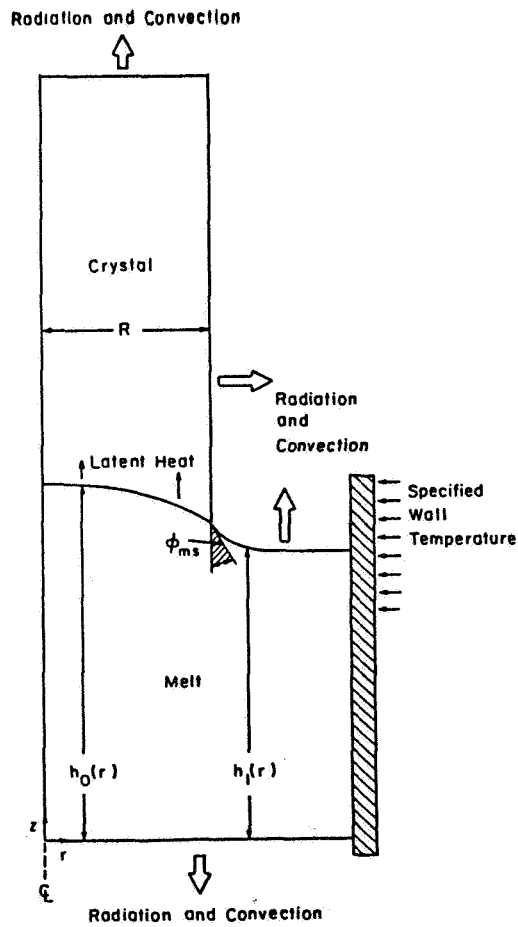
CAPILLARITY AND INTERFACES

melt-solid interface  $B(r, h_0(r)) = 1$

meniscus 
$$\frac{\frac{d^2 h_1}{dr^2}}{\left[1 + \left(\frac{dh_1}{dr}\right)^2\right]^{3/2}} + \frac{\frac{dh_1}{dr}}{r \left[1 + \left(\frac{dh_1}{dr}\right)^2\right]^{1/2}} = E\sigma (h_1(r) - \lambda)$$

radius 
$$\left. \frac{dh_1}{dr} \right|_R = \tan(\phi_{ms} - 90^\circ)$$

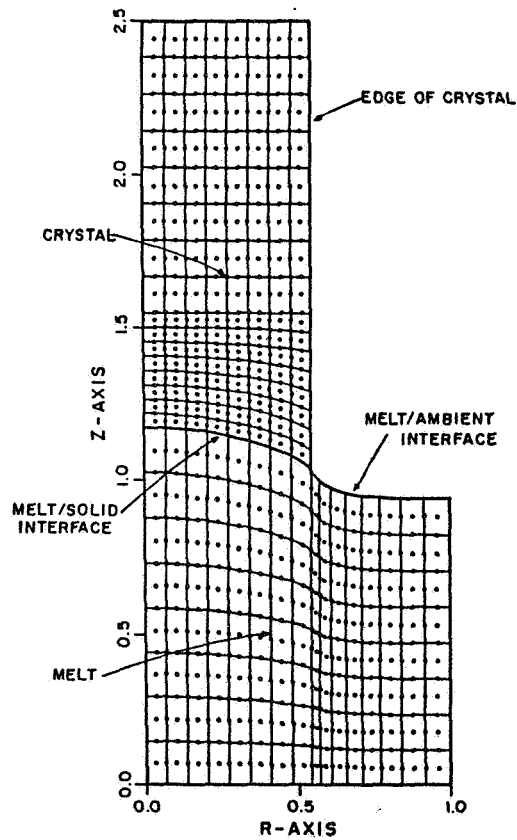
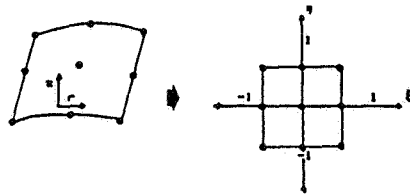
volume constraint 
$$\int_0^R h_0(r) r dr + \int_R^1 h_1(r) r dr = V_m / 2\pi$$



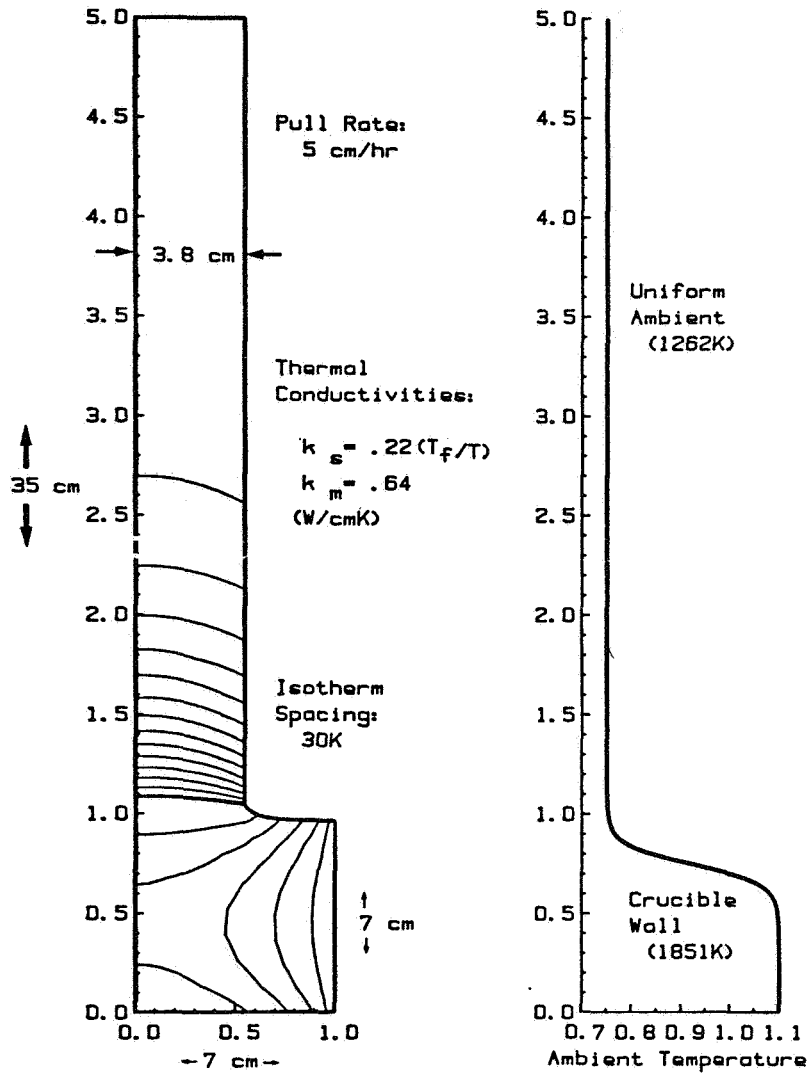
## FINITE ELEMENT/NEWTON METHOD

- Piecewise-continuous polynomials used to approximate temperature field (2d) and interface shapes (1d)
- Adaptive mesh defined by free boundaries
- Galerkin method and elemental isoparametric mapping used to generate set of nonlinear algebraic equations
- Newton's method used to solve equation set, giving quadratic convergence to solution

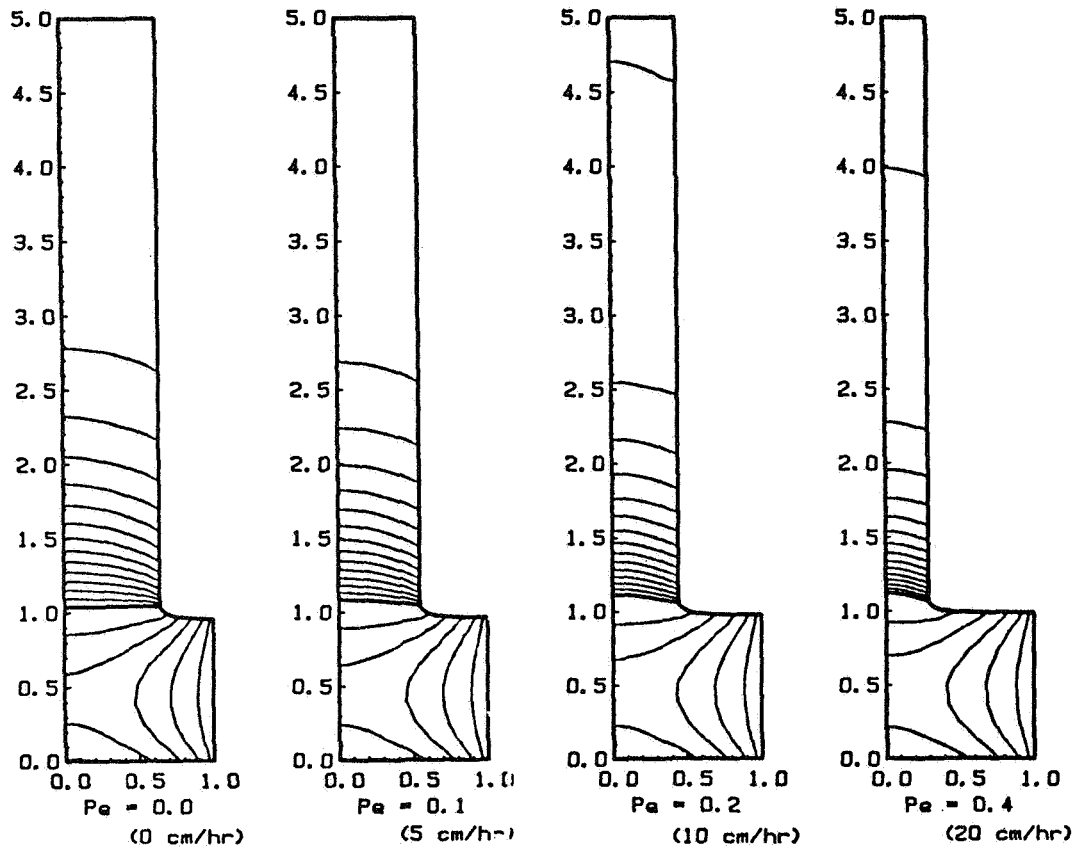
## ISOPARAMETRIC MAPPING



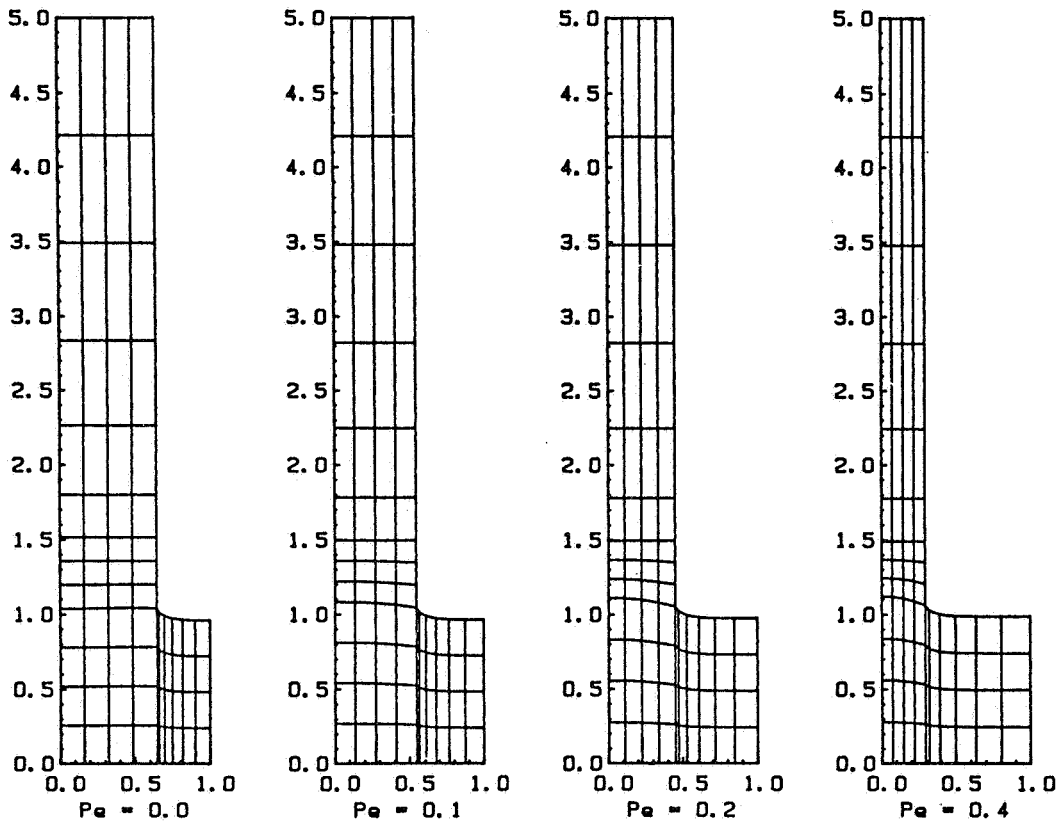
# Parameters—Silicon



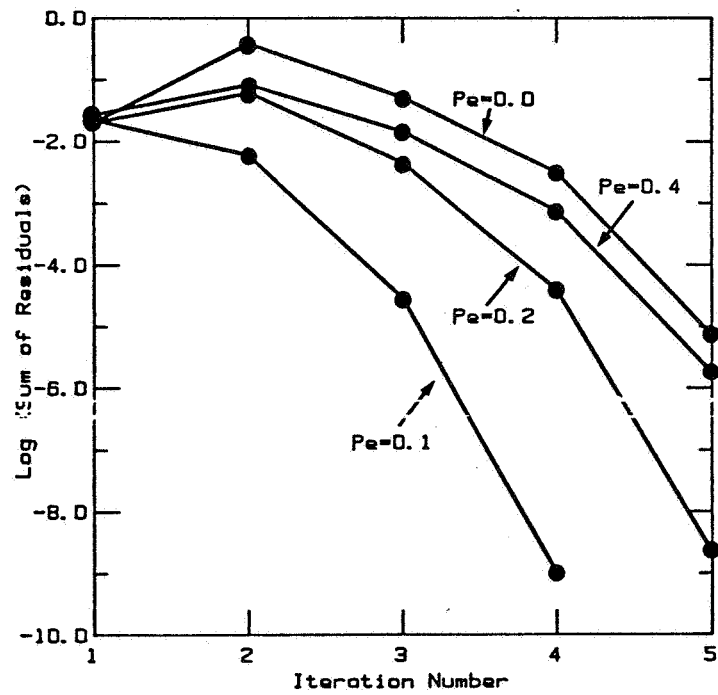
# Changes in Pull Rate



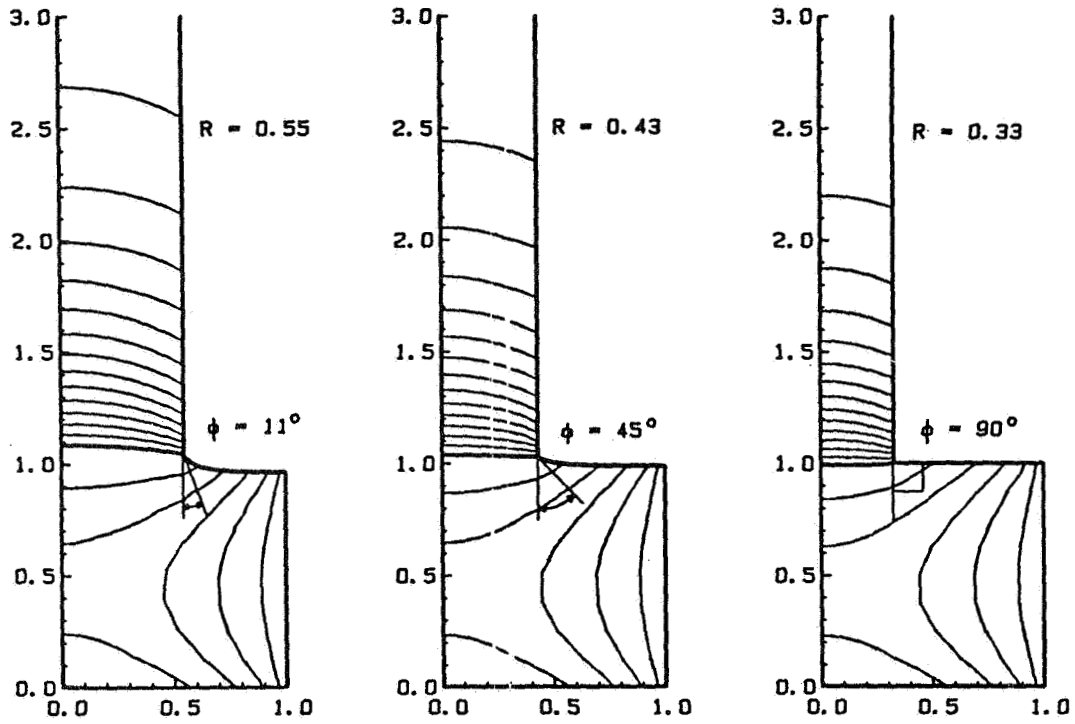
## Finite-Element Meshes for Different Pull Rates



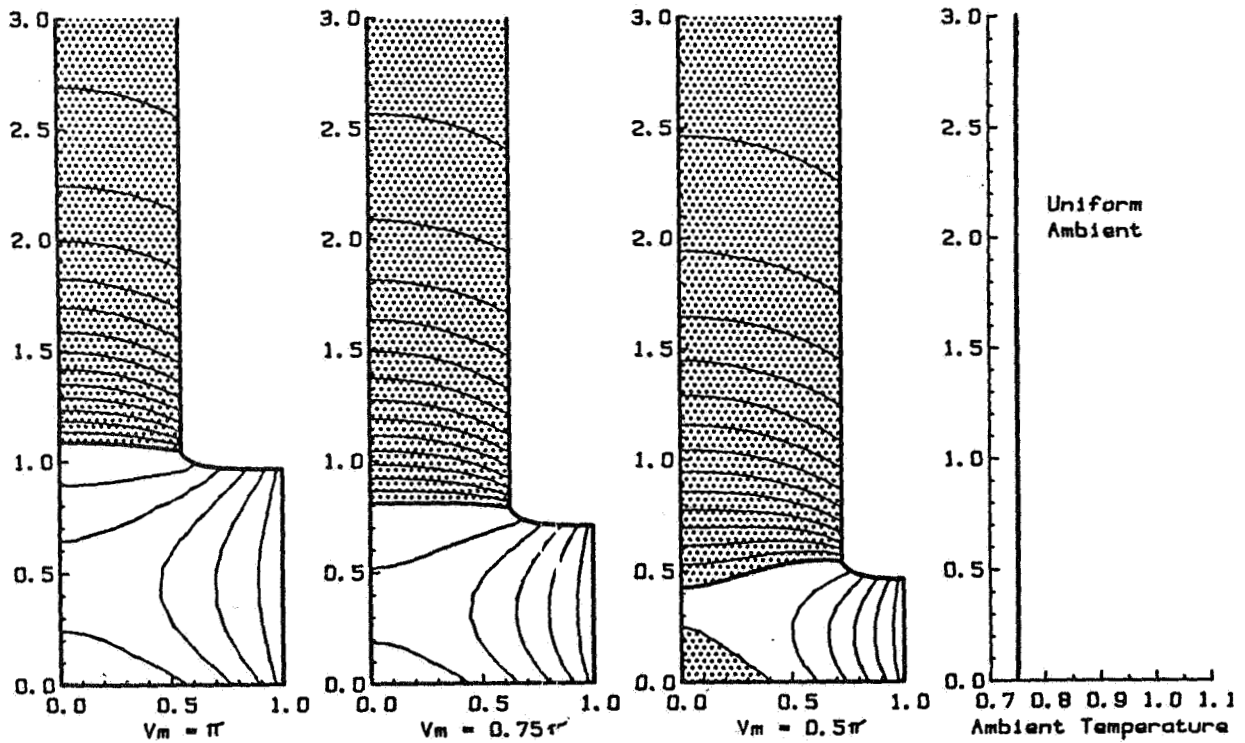
## Convergence Behavior



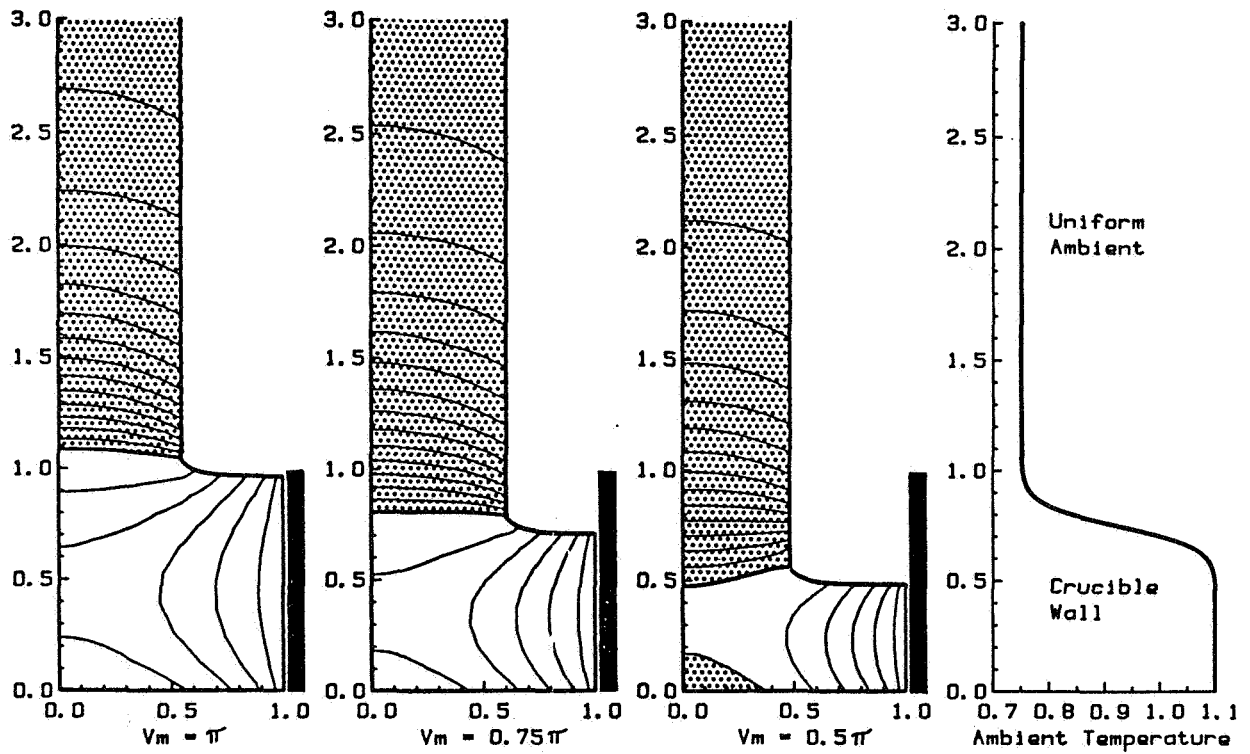
## Variations in Equilibrium Angle



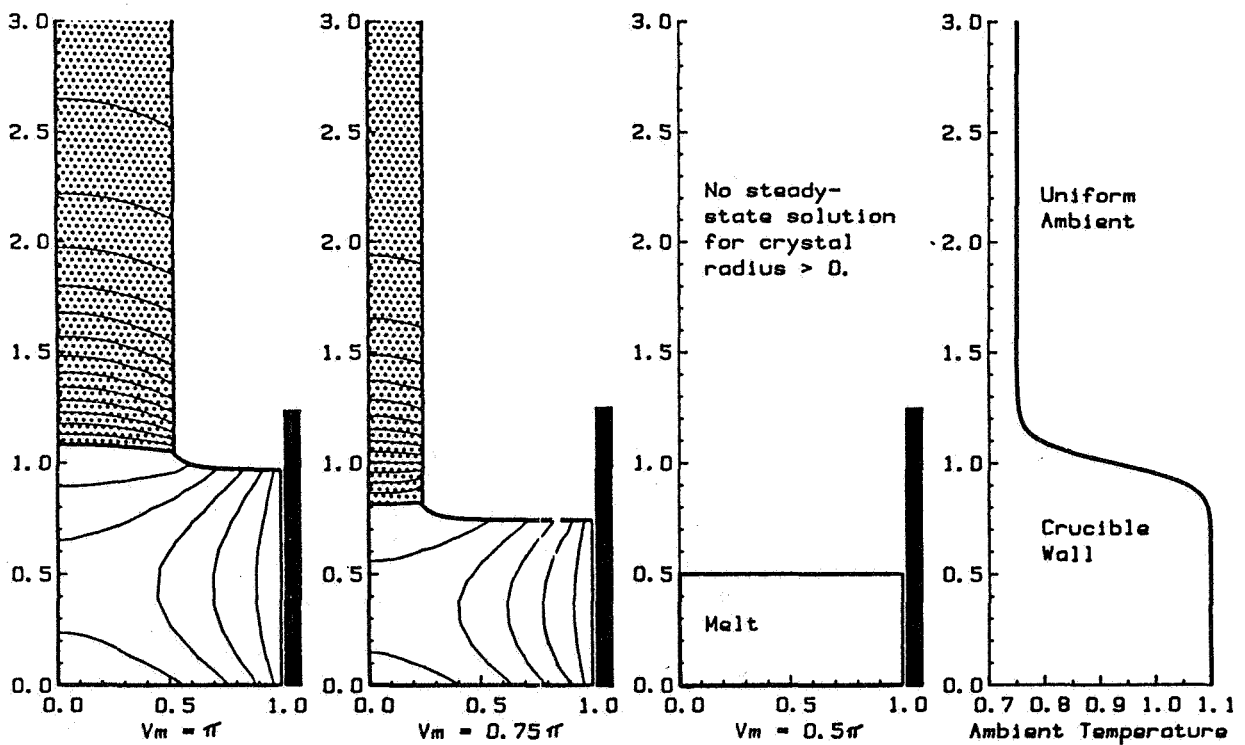
## Decreasing Melt Volume—Uniform Ambient



### Decreasing Melt Volume—Shallow Crucible

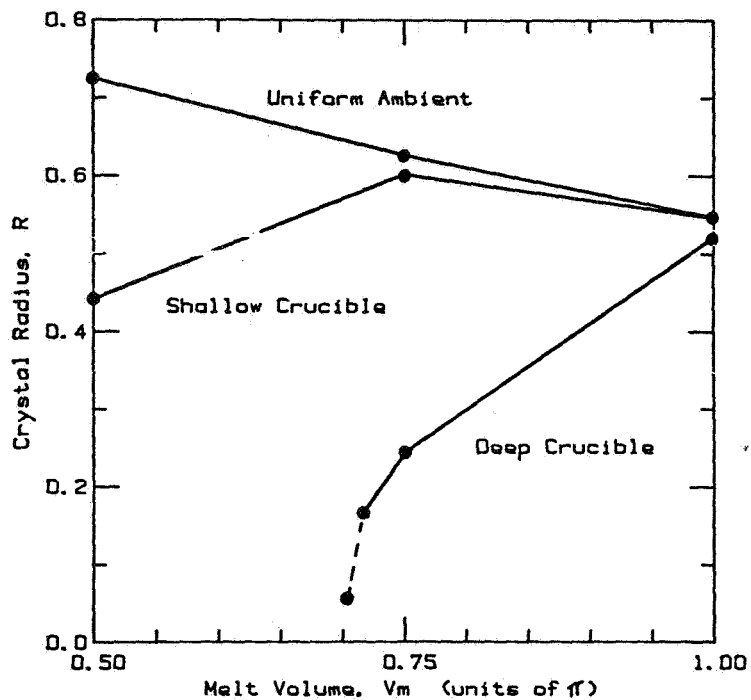


### Decreasing Melt Volume—Deep Crucible





# Radius as a Function of Melt Volume



## DISCUSSION

ELWELL: Is it too complicated to plug convection in the Czochralski system?

BROWN: It depends on your goal. We are working on convection, and we are working on convection in other systems that are quite a bit simpler than this. To come up with a good algorithm for doing convection in a large Czochralski system means you have to handle convection that is in the never-never land between laminar and turbulent flow, which is essentially chaotic. It is too complicated at present to plug that kind of convection model into a calculation like this and hope to get back out some kind of a control strategy. Those are supercomputer-type calculations, unless you are willing to put in a turbulent model, which we are not willing to do right now.

DUDUKOVIC: You use a static value of the contact angle in all of your calculations, which is of course fine because presumably the pulling rates are so low. What do you do about the value of that angle in presence of the Marangoni effect?

BROWN: If you really believe that is a thermal physical property of what is right down at the intersection between melt/solid and gas then you would believe that the bulk fluid mechanics should not have a lot of effect on them. That concept has been shown to have been true not in solidification systems but in normal wetting conditions as long as the contact line is not moving at high rates of speed.

DUDUKOVIC: At the moment that's the best assumption one can make, but isn't there still some doubt about it under dynamic conditions?

BROWN: If it's a microscopic property of the physics of the tri-junction I don't think there is any scaling you can do to show that a bulk flow can affect it. For example, gravity cannot affect it. The same kind of argument you would use to say that the surface tension is independent of gravity is used and, in fact it's one order of magnitude worse.

KIM: In your aluminum segregation study, what was the effective segregation coefficient that you have measured?

BROWN: One.

KIM: What was the solid boundary layer thickness?

BROWN: There is no boundary layer thickness because in the EFG system that is a big problem. The flow field in the die is well developed and there is no effective segregation in the system. Any aluminum that comes up through that die has to go into the crystal. It has no place else to go.

KALEJS: It is quite true for  $K_{eff}$  equal to unity that there are a lot of impurities that ended up very close to the meniscus, but this is

true for a lot of the shaped crystal growth systems like web. We have looked at this and found that the change in surface tension with impurity concentration goes opposite to the temperature difference, so you may expect some kind of cancellation due to impurity effects, particularly in  $K_{\text{eff}}$  equal to unity where a lot of impurities do end up in the meniscus.

SUREK: Regarding Professor Dudukovic's question: the contact angle was determined over many orders of magnitude of growth rate, essentially from zero growth rate to very fast growth rate without much variation, so it seems to be a property of the silicon at a triple junction. My question is if you showed points or regions where there is no existence of a steady-state solution, would that be the limit of stability, in your opinion?

BROWN: The EFG calculations give you the growth-rate limit for steady-state solutions for growing a ribbon with that die at that  $K_{\text{eff}}$ . We had not found similar limits in the Czochralski system, but I think all one needs to do is play around with the thermal ambient to actually find growth-rate limits in that system also. I don't think people worry about it as much because they concentrate more on high-quality material and less on growth speed.

SUREK: In what system was it that you found no solution?

BROWN: In the Czochralski system. Essentially that's associated with just excessive heat transfer from the ambient directly into the crystal, which essentially just blocks up the heat so that you can't get it out of the melt. We are not sure whether or not that is essentially just the crystal growing to zero diameter or whether or not there really is a limit point there. We haven't refined that enough to find out.

WITT: How do you handle the complication that normally is encountered when you grow dislocation-free silicon? In conventional growth, you end up with the peripheral interface facet, which places the critical portion of the crystal into a supercooled state, and we know that you lose, for one reason or another, the dislocation-free growth configuration. The instantaneous consequence is a significant change in crystal diameter, which means that effectively the growth does not occur in critical portions, particularly at the periphery, which is a critical point way away from the melting point. My second question: a very important element is the rate of crucible consumption or the melt/crucible interaction or the mass transfer related to oxygen and impurities. Are you looking at these factors?

BROWN: We have not been. Obviously, if you take the same segregation model we can dissolve the crucible with it if you want. We have not been doing it. In answer to your first question, interface faceting is a fantastic piece of physics that could be put in here if I knew the orientation and undercooling law for doing it. There's nothing that keeps us from putting in a faceted growth mode at the interface. It would be very interesting to do, and there are some mathematical

reasons why it's very nice to do in the finite-element formulation. You could very easily come up with an interface that has facets along part of it and equilibrium growth on other parts. If someone would stick their neck out and give me the undercooling law I'd love to do it, because I think it would be very interesting. I think that introduces an additional non-linearity, which I think can give you catastrophic behavior, which is what you referred to with the loss of the facet in the growth of the crystal. Do you know of someone that has written down this nucleation law?

WITT: It is still very controversial in details. The theory is worked out.